Clinopyroxenes of the gabbro cumulates of the Kap Edvard Holm complex, east Greenland

By W. A. Deer and D. Abbott[1]

Department of Mineralogy and Petrology, Cambridge

Summary. The major part of the Kap Edvard Holm complex consists of two series of conspicuously banded gabbroic rocks. The primary minerals of both lower and upper layered series show a progressive change in composition, from higher to lower temperature phases, with increasing height in the complex. Minor fluctuations in the differentiation of the two series occur but the division of the layered rocks into the lower and upper series is based on abrupt and major changes in the compositions of the pyroxenes, olivine and plagioclase. This break is correlated with the injection of a large volume of undifferentiated magma which occurred after much of the lower layered series had consolidated, and from which the rocks of the upper layered series were formed. Twelve pyroxenes, five from the lower and seven from the upper layered series have been analysed; the relationships between their optical properties and chemical composition, and between the cell parameters and composition are considered. The crystallization trend of the pyroxenes is compared with that of the Skaergaard calcium-rich pyroxenes; it is suggested that the restricted enrichment in iron shown by the Kap Edvard Holm pyroxenes may be related to the higher water-vapour pressures which prevailed during much of the period of crystallization.

THE Kap Edvard Holm complex is situated on the west side of Kangerdlugssuaq fjord, east Greenland (68° 5′ N., 31° 31′ W.). The complex is some 15 km from the Skaergaard intrusion (Wager and Deer, 1939) situated on the east side of the fjord, and lies immediately to the south of the alkaline Kangerdlugssuaq intrusion (Wager, 1965).

The complex extends northwards from Kap Edvard Holm Mountain to the Hutchinson glacier (fig. 1), and occupies an area of approximately 300 km^2, much of which is covered by small glaciers and ice fields. To the west the igneous rocks are in contact with the gneisses of the metamorphic complex (Wager, 1934), and to the south with basalts of Eocene age. Gabbroic rocks extend northwards for an unknown distance beneath Hutchinson glacier, and it is probable that gabbros south of Andrup Mountain and along the coast north of Kap Deichman, form part of the Kap Edvard Holm complex. From the general structure of the complex it is possible that these gabbros represent rocks lower in the

[1] Present address: Research and Productivity Council, Fredericton, Canada.

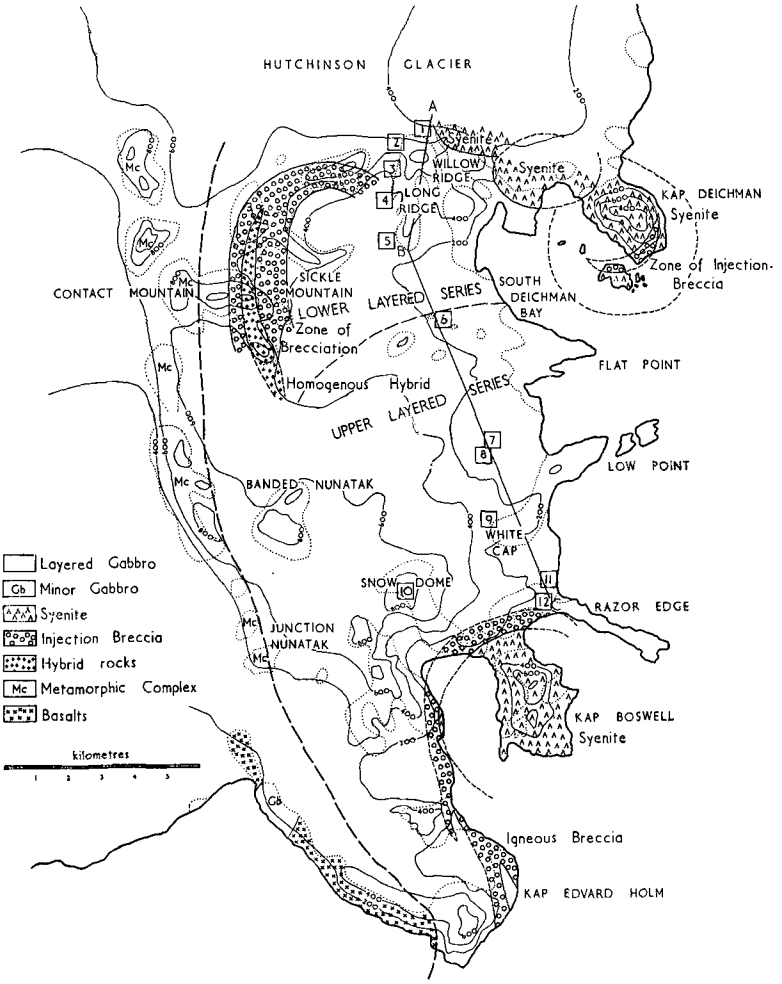

FIG. 1. Map of the Kap Edvard Holm Complex, east Greenland. Location of the rocks from which the pyroxenes have been analysed are shown by numbers in squares.

complex than those south of Willow Ridge, but because the relationship of these rocks to those of the main part of the complex is not known precisely they are not considered here.

The major part of the complex consists of two series of gabbroic rocks, a lower layered and an upper layered series. The lower layered series in the northern part of the complex shows conspicuous rhythmic banding.

The rocks are remarkably free from xenoliths and along the 2-mile long, 1000 ft high exposure on Long Ridge only one xenolith, a rock belonging to the metamorphic complex, was observed. The upper layered series which occupy the central and southern parts of the complex is also well banded, the banding is more variable in character and includes rhythmic, gravity, and 'inch scale layering' (Hess, 1960). The cumulates (Wager *et al.*, 1960) of the upper layered series contain many xenoliths, the most conspicuous of which have an anorthositic composition (modal plagioclase 90–98 vol. % An_{70}–An_{73}), and which are considered to have been derived from the disruption of the earlier formed cumulates of the lower layered series. The anorthositic xenoliths, as indeed other xenoliths, which include cumulates of gabbro composition, rocks of the metamorphic complex as well as the basalts, are particularly abundant in the lowest rocks of the upper layered series.

Although the presence of a large number of xenoliths is the most conspicuous feature in the field by which the upper layered series is distinguished from the lower layered series, the division between the two series is based on abrupt and major changes in the compositions of the cumulate minerals which occur at a height of 3850 m (fig. 2). In the lower layered series there is a generally progressive change in the compositions of the three main cumulate minerals, from higher to lower temperature phases. That minor breaks in the progressive differentiation of the series have occurred is indicated particularly by fluctuations in the compositions of the plagioclases and by the character of their zoning. These compositional changes are considered to result from minor influxes of undifferentiated magma. The phase changes on which the separation of the layered series into a lower and upper division is based are of a different order of magnitude, and the three primary silicate phases in the lowest cumulates of the upper layered series have compositions which indicate higher crystallization temperatures than the minerals which occur in any of the rocks of the lower layered series. These major changes in mineral compositions and their coincidence with the appearance of abundant xenoliths is considered to be due to a large-scale injection of new magma which took place after much of the lower series liquids had crystallized and consolidated.

Additional, although not conclusive, evidence of the relative independence of the lower and upper layered series is obtained from the disposition of the banding in the two series. In the Willow and Long Ridge area of the lower layered series the banding dips between 30° and 45° SW., in the central area between 45° and 50° SE., and on Contact

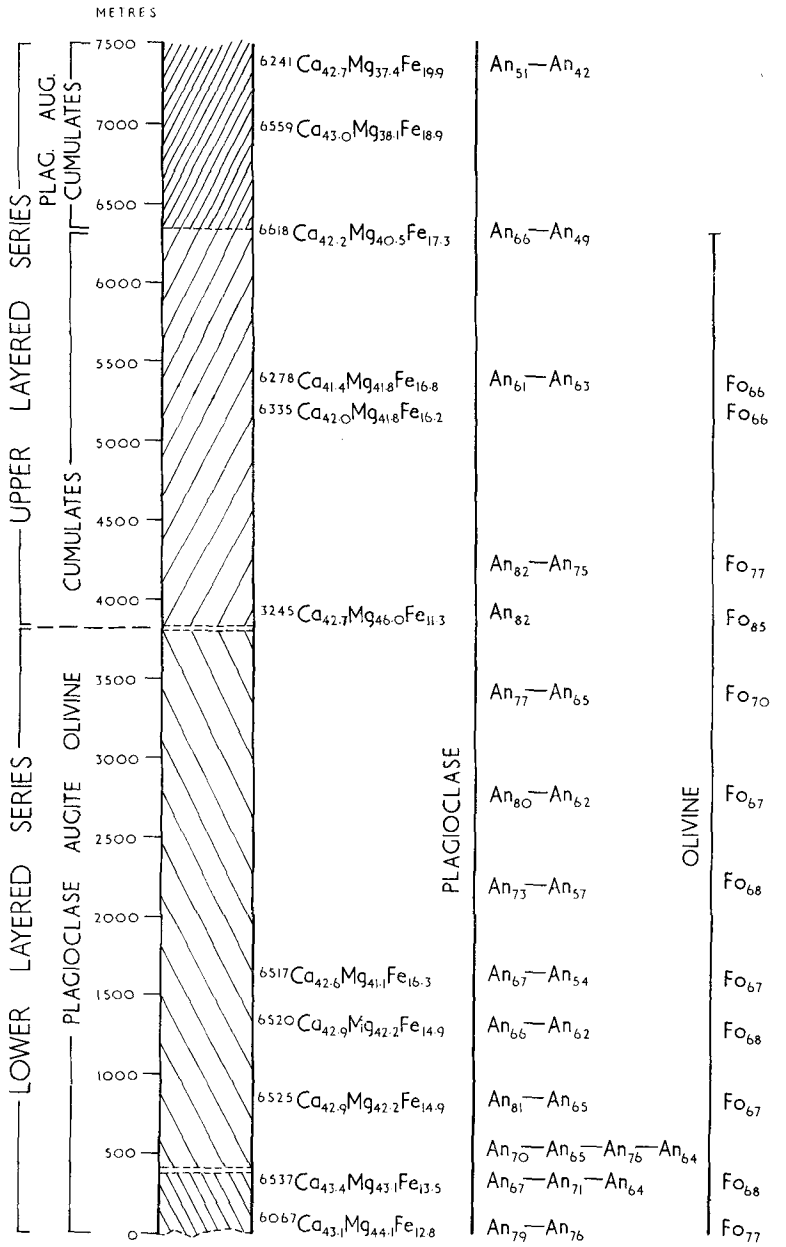

FIG. 2. The relative heights of rocks of the lower and upper layered series from which pyroxenes have been analysed, together with compositions of plagioclase and olivines determined respectively from optical properties and $d_{(130)}$ spacings.

Mountain between 45° and 55° W.; the focus of the banding is thus located approximately at the medial point between Flat Point and Sickle Mountain. In the upper layered series the dips of the banding follow a somewhat different pattern. At Flat Point the dips of the banding are between 20° and 35° S.; in the Low Point area the dips are predominantly southerly but the dip angle is lower and in the range 15° to 25°. Along the western margin the direction of the banding is east at angles between 50° and 70°, in the Snow Dome area the banding dips 40° ESE. At Kap Edvard Holm in the extreme south the banding dips 50° NE., and the probable focus of the banding is somewhat south of Razor Edge. Although the banding in both layered series, but particularly in the more extensive upper unit, is consistent with the broad pattern of steeper dips at the margins and a gradual flattening of the banding towards the centre, irregularities of some magnitude occur. These can, however, in many instances be related to the enechelon form of the regional crustal flexure and dyke swarm (Wager and Deer, 1938) which post-date the formation of the basic rocks of the Kap Edvard Holm complex.

Subsequent to the intrusion of the dyke swarm, the syenites and injection breccias of Kap Boswell, Kap Deichman, North and South Willow Ridge, and Sickle Mountain were emplaced. The syenites include arfvedsonite–aegirine, ferrohortonolite–hedenbergite and hornblende–biotite syenites, and nordmarkite. The syenite contacts with the gabbros are sharp, and are vertical or steeply dipping outwards. Brecciation of the basic rocks is most intense at the western end of Sickle Mountain, and here the syenite veining extends into the rocks of the metamorphic complex. Here the central portion of the wide breccia zone consists of a rock which, although of largely homogeneous character, is of hybrid origin due to contamination of a syenitic magma by basic material prior to its emplacement.

General mineralogy of the gabbro cumulates

Twelve pyroxenes, five from the lower, and seven from the upper layered division have been analysed (tables I and IV). The heights of the pyroxenes in the layered series and their Ca:Mg:Fe ratios are shown in fig. 2. The compositions of the other two main cumulate phases are also detailed in the figure; plagioclase compositions were determined by an extinction method using a four-axis universal stage (Turner, 1947), and the olivine compositions from $d_{(131)}$ spacings (Yoder and Sahama, 1957). In addition to plagioclase, pyroxene, and olivine, titanomagnetite

and ilmenite are the only other cumulate minerals which occur in appreciable quantities. Titanomagnetite is present in greater amount than ilmenite. There is no systematic change in the titanomagnetite: ilmenite ratio with height, but the rocks of the lower layered series generally contain more magnetite relative to ilmenite, ratio average 2·7, than the upper layered series cumulates, ratio average 2·1. Orthopyroxene is rarely present in the Kap Edvard Holm cumulates and is restricted to occasional narrow reaction rims around crystals of olivine.

In most of the rocks of the lower layered series some late intercumulus crystallization is represented by chlorite, serpentine, clinozoisite, and prehnite, and similar hydrous phases are present in the higher cumulates of the upper layered series. In the upper series in particular there is a notable increase in the amount of these minerals with increasing height in the series. In some of the highest cumulates, e.g. 6559, calcite and quartz in small quantities also occur as products of crystallization from the intercumulus liquids. Other primary minerals occurring in small amounts include biotite, hastingsitic amphibole, and apatite, and the sulphides, chalcocite, bornite, and pyrrhotite.

The pyroxenes from the lower layered series are all associated with plagioclase and olivine, and the three main cumulate phase occur throughout this series. In the upper layered series, however, plagioclase augite olivine orthocumulates form only the lower 2500 m. Above the 6400 m level olivine is not present and pyroxenes 6618, 6559, and 6241 (table IV, nos. 9, 10, 11) occur in plagioclase augite orthocumulates. The ferroaugite (table IV, no. 12) is from an iron-rich granophyre which, although closely associated with the plagioclase augite orthocumulates of the upper series, did not form in situ by crystal accumulation.

Physical and optical properties of the pyroxenes

The majority of the augites are pale brown in colour, but some are pale greenish or pinkish brown. Opaque inclusions, either as thin needle-like rods or as small blebs, occur in the augites of both the lower and upper layered series, but are more commonly developed in the cumulates of the lower series. The needles, usually less than 0·1 mm, but occasionally as much as 1·5 mm in length are oriented mainly in the (010) plane of the crystals but a smaller number occur in a plane normal to (010). The ubiquitous presence of these inclusions in the augites of the lower layered series suggests that they are the result of an exsolution with falling temperature and increasing water-vapour pressure. The augites in the metamorphosed cumulates adjacent to the North and

TABLE I. Chemical and spectrographic analyses of pyroxenes of the lower layered series

	(6067) 1	(6537) 2	(6525) 3	(6520) 4	(6517) 5
SiO_2	49·69	50·25	50·56	50·61	50·89
TiO_2	1·05	1·41	0·83	0·93	1·10
Al_2O_3	3·95	3·83	3·40	4·01	3·06
Fe_2O_3	1·75	1·95	1·46	0·97	1·35
Cr_2O_3	0·75	0·24	—	—	—
FeO	6·25	6·34	7·52	7·98	8·53
MnO	0·17	0·19	0·14	0·25	0·28
MgO	15·35	14·85	14·79	14·51	14·24
CaO	20·91	20·77	20·95	20·55	20·48
Na_2O	0·49	0·41	0·50	0·42	0·39
K_2O	0·01	0·01	0·03	0·01	0·01
H_2O^+	0·03	—	0·13	—	—
Total	100·40	100·25	100·31	100·24	100·33
Semi-quantitative spectrographic analyses (ppm)					
Ga^{+3}	5	5	5	5	5
Cr^{+3}	10 000	2160	1000	850	220
V^{+3}	760	480	420	420	480
Mo^{+4}	1	tr	1	1	1
Li^{+1}	3	1	1	1	7
Ni^{+2}	250	220	100	100	100
Co^{+2}	46	46	46	46	46
Cu^{+2}	5	100	22	100	100
Sc^{+3}	180	100	125	125	125
Zr^{+4}	46	28	46	46	100
Y^{+3}	22	22	25	32	32
La^{+3}	tr	tr	tr	tr	tr
Sr^{+2}	32	15	15	18	32
Pb^{+2}	tr	tr	55	tr	10
Ba^{+2}	20	tr	tr	tr	5
Rb^{+1}	tr	tr	tr	tr	tr

Key to Tables I, II and III

1. Augite from plagioclase augite olivine cumulate (6067, 50 m), West Willow Ridge.
2. Augite from plagioclase augite olivine cumulate (6537, 350 m), Long Ridge.
3. Augite from plagioclase augite olivine cumulate (6525, 800 m), Long Ridge.
4. Augite from plagioclase augite olivine cumulate (6520, 1350 m), Long Ridge.
5. Augite from plagioclase augite olivine cumulate (6517, 1600 m), Long Ridge.

Analyses 1, 2, 4, 5 by J. H. Scoon. Analysis 3 by D. Abbott.

South Willow Ridge syenites contain a larger number of the bleb-like inclusions and indicate that further exsolution, which gave rise to a metamorphic clouding, accompanied their reheating. A detailed analysis of the needles and blebs has not been attempted but a preliminary

TABLE II. Formulae, on the basis of six oxygen atoms, of pyroxenes of the lower layered series

	1	2	3	4	5
Si	1·841	1·859	1·879	1·877	1·893
Al	0·159	0·141	0·121	0·123	0·107
Al	0·016	0·027	0·028	0·042	0·027
Ti	0·029	0·039	0·023	0·026	0·031
Fe^{+3}	0·048	0·054	0·041	0·027	0·038
Cr	0·022	0·007	—	—	—
Mg	0·830	0·819	0·819	0·802	0·789
Fe^{+2}	0·194	0·196	0·234	0·248	0·265
Mn	0·005	0·006	0·004	0·008	0·009
Ca	0·830	0·823	0·834	0·817	0·816
Na	0·035	0·029	0·036	0·030	0·028
K	—	—	0·001	—	—
% $[Al]^4$	8·0	7·0	6·0	6·1	5·3
% $[Al]^6$	0·8	1·3	1·4	2·1	1·3
			Atomic %		
Ca	43·1	43·4	42·9	42·9	42·6
Mg	44·1	43·1	42·2	42·2	41·1
(Fe^{+2}, Fe^{+3}, Mn)	12·8	13·5	14·9	14·9	16·3

TABLE III. Optical properties and cell dimensions of pyroxenes of the lower layered series

	1	2	3	4	5
α	1·692	1·692	1·692	1·692	1·693
β	1·705	1·705	1·705	1·705	1·705
γ	1·719	1·719	1·719	1·719	1·720
$2V_\gamma$	51°	50°	52°	52°	48°
$\gamma:z$	43°	42°	42°	45°	42°
D	3·33	3·35	3·35	—	3·38
a (Å)	9·747	9·743	9·749	9·751	9·751
b (Å)	8·922	8·928	8·926	8·936	8·936
c (Å)	5·234	5·234	5·232	5·241	5·233
β	73° 43′	73° 43′	73° 47′	73° 52′	73° 49′
$a \sin \beta$	9·356	9·352	9·361	9·367	9·365
vol. (Å^3)	436·9	437·0	437·2	438·7	437·9

examination by electron probe has shown that they consist principally of iron with smaller amounts of titanium. The metamorphosed clouded crystals are bleached and their initial brown colour is thus probably related to their iron content, the subsequent exsolution of which resulted in loss of colour.

Preliminary estimates of the refractive indices of most of the augites of both the lower and upper layered series did not reveal significant differences between them, and subsequent measurements to an accuracy

of $\pm 0{\cdot}001$, confirmed, except for pyroxenes 6 and 12, that the variations are small. In fig. 3 the β-indices are plotted on the curves showing variation of optical properties with chemical composition of clinopyroxenes in part of the system $CaMgSi_2O_6$–$CaFeSi_2O_6$–$MgSiO_3$–$FeSiO_3$ (Brown and Vincent, 1963). It is evident from the figure that the measured β indices (except for ferroaugite, 6247) are approximately 0·01 higher than would be predicted from the compositions of the augites of the Kap Edvard Holm gabbro cumulates. A poorer correlation between measured and indicated values is obtained from the earlier curves constructed by Hess (1949) and later modified by Muir (1951); on the basis of these curves the values of the Kap Edvard Holm augites are some 0·015 higher than is indicated by their Mg:Fe ratios.

The augites of the layered rocks have optic axial angles between 48° and 52°, but there is little correlation between the values of $2V$ and the replacement of Mg by Fe. Compared with the optic axial angles of Skaergaard augites with similar Mg:Fe ratios, $2V_\gamma$ of the Kap Edvard Holm pyroxenes are approximately 5° higher, a difference which may be due to the higher Ca content of the Kap Edvard Holm pyroxenes. Augites 6517, 6618 and 6241 give $2V_\gamma$ values of 48–49° and 52° on different parts of the same grain as well as on individual crystals in thin section. The augites show no primary zoning, but since the higher value in each case is confined to slightly turbid crystals, or to the turbid parts of otherwise clear crystals, they are probably related to incipient compositional changes, and it is possible that the higher optic axial angles in these pyroxenes are associated with the conversion of some ferrous to ferric iron.

The curves relating optical properties to chemical composition constructed by Hess, Muir, and Brown are based on the assumption that constituents other than Ca, Mg, and Fe are present in approximately the following amounts, expressed as oxides: Al_2O_3, 3 %, Fe_2O_3, 1·5 %, TiO_2, 0·4 %, and Na_2O, 0·4 %. A comparison of the mean values of these oxide percentages in the Kap Edvard Holm, Skaergaard, and Stillwater clinopyroxenes shows that Al_2O_3 is the only oxide in which the analyses of the Kap Edvard Holm pyroxenes differ significantly from those of the augites of both the Skaergaard and Stillwater rocks (4·2, 2·7, and 3·0 wt. % respectively). In addition the mean TiO_2 value of the analyses of the Kap Edvard Holm augites is markedly higher than that of the Stillwater clinopyroxenes (1·1 and 0·4 wt. % respectively).

The study, by Zvetkov (1945), of a series of synthetic solid solutions, from pure diopside to diopside containing 40 mol. % $CaAl_2SiO_6$, showed

TABLE IV. Chemical and spectrographic analyses of pyroxenes of the upper layered series

	(3245) 6	(6335) 7	(6278) 8	(6618) 9	(6559) 10	(6241) 11	(6247) 12
SiO_2	49·20	49·65	49·78	50·51	48·17	48·84	44·22
TiO_2	0·89	0·91	1·09	0·76	1·01	1·46	2·27
Al_2O_3	5·56	4·34	4·89	3·41	6·10	5·40	6·46
Fe_2O_3	1·00	1·92	1·41	1·30	3·61	1·35	1·48
Cr_2O_3	0·46	—	—	—	—	0·03	—
FeO	5·96	8·09	8·64	9·23	7·77	10·33	19·36
MnO	0·12	0·17	0·19	0·19	0·20	0·19	0·73
MgO	15·90	14·49	14·11	13·89	12·73	12·43	6·74
CaO	20·50	20·21	19·45	20·11	19·97	19·64	17·79
Na_2O	0·33	0·41	0·67	0·37	0·32	0·45	0·47
K_2O	0·01	0·01	0·04	0·03	0·02	0·07	0·08
H_2O^+	0·15	0·11	0·04	0·21	0·21	0·08	0·41
Total	100·08	100·31	100·31	100·01	100·11	100·27	100·01
	Semi-quantitative spectrographic analyses (ppm)						
Ga^{+3}	2	—	9	5	—	12	20
Cr^{+3}	5000	—	1000	850	—	465	32
V^{+3}	420	—	760	420	—	420	32
Mo^{+4}	1	—	1	1	—	2	2
Li^{+1}	1	—	1	1	—	4	10
Ni^{+2}	1000	—	150	100	—	56	10
Co^{+2}	100	—	46	46	—	46	22
Cu^{+2}	46	—	10	32	—	10	22
Sc^{+3}	85	—	180	100	—	180	180
Zr^{+4}	28	—	36	56	—	100	100
Y^{+3}	12	—	22	46	—	46	56
La^{+3}	tr	—	tr	tr	—	tr	tr
Sr^{+2}	32	—	18	15	—	70	40
Pb^{+2}	tr	—	tr	tr	—	tr	tr
Ba^{+2}	20	—	tr	tr	—	20	tr
Rb^{+1}	tr	—	tr	tr	—	tr	tr

Key to Tables IV, V and VI

6. Augite from plagioclase augite olivine cumulate (3245, 3900 m), Z Nunatak.
7. Augite from plagioclase augite olivine cumulate (6335, 5150 m), Linear Nunataks.
8. Augite from plagioclase augite olivine cumulate (6278, 5350 m), Aeroplane Nunatak.
9. Augite from plagioclase augite cumulate (6618, 6400 m), Wall Rock.
10. Augite from plagioclase augite cumulate (6559, 7000 m), Snow Dome.
11. Augite from plagioclase augite cumulate (6241, 7350 m), South Low Point Bay.
12. Ferroaugite from ferroaugite granophyre (6247), West Razor Edge.

Analyses 6, 7, 9, 10, 11, 12 by W. A. Deer and J. Johnson. Analysis 8 by D. Abbott.

TABLE V. Formulae, on the basis of six oxygen atoms, of pyroxenes of the upper layered series

	6	7	8	9	10	11	12
Si	1·819	1·849	1·851	1·892	1·805	1·833	1·753
Al	0·181	0·151	0·149	0·108	0·195	0·167	0·247
Al	0·061	0·030	0·065	0·042	0·075	0·072	0·055
Ti	0·025	0·026	0·030	0·021	0·028	0·041	0·068
Fe^{+3}	0·028	0·054	0·039	0·036	0·102	0·038	0·044
Cr	0·014	—	—	—	—	0·001	—
Mg	0·876	0·805	0·782	0·775	0·711	0·695	0·398
Fe^{+2}	0·184	0·252	0·269	0·289	0·244	0·324	0·642
Mn	0·004	0·005	0·006	0·006	0·006	0·006	0·025
Ca	0·812	0·807	0·775	0·807	0·802	0·790	0·756
Na	0·024	0·029	0·048	0·027	0·023	0·033	0·036
K	—	—	0·002	0·001	0·001	0·003	0·004
$[Al]^4$	9·0	7·5	7·4	5·4	9·7	8·3	12·3
$[Al]^6$	3·0	1·5	3·2	2·1	3·7	3·6	2·7
			Atomic %				
Ca	42·7	42·0	41·4	42·2	43·0	42·7	40·5
Mg	46·0	41·8	41·8	40·5	38·1	37·4	21·4
(Fe^{+2}, Fe^{+3}, Mn)	11·3	16·2	16·8	17·3	18·9	19·9	38·1

TABLE VI. Optical properties and cell dimensions of the pyroxenes of the upper layered series

	6	7	8	9	10	11	12
α	1·687	1·692	1·693	1·691	1·693	1·695	1·706
β	1·699	1·705	1·706	1·705	1·706	1·707	1·716
γ	1·714	1·719	1·719	1·719	1·721	1·721	—
$2V_\gamma$	52°	51°	49°	51°	50°	48°	58°
$\gamma:z$	—	43°	42°	42°	42°	42°	43°
D	—	3·37	3·38	3·37	3·38	—	—
a (Å)	9·744	—	9·756	9·752	—	9·761	—
b (Å)	8·923	—	8·936	8·941	—	8·937	—
c (Å)	5·236	—	5·232	5·235	—	5·266	—
β	73° 26′	—	73° 44′	73° 44′	—	73° 42′	—
$a \sin \beta$	—	—	9·365	9·362	—	9·369	—
vol. (Å^3)	—	—	437·8	438·2	—	440·9	—

that there is a linear relationship between the refractive indices of this series of compositions and the content of Al, and that the replacement of 20 % Si and Mg by $[Al]^4$ and $[Al]^6$ is accompanied by an increase of approximately 0·02 in both the α and γ indices. Data bearing on the relative effects of tetrahedrally and octahedrally co-ordinated Al on the refractive indices of clinopyroxenes is both scanty and conflicting. Comparison of the mean percentages of tetrahedrally co-ordinated Al in the Kap Edvard Holm, Skaergaard, and Stillwater augites (7·3, 4·1, and

4·4 % respectively), however, indicates, contrary to Hori's (1954) conclusion, that tetrahedrally co-ordinated Al leads, in the pyroxene structure, to an increase in refractive indices. The observed increase in the Kap Edvard Holm relative to the Skaergaard augites is, however, not as great as would be anticipated from Zvetkov's data on the synthetic solid solution series $CaMgSi_2O_6$–$(6CaMgSi_2O_6 \cdot 4CaAl_2SiO_6)$.

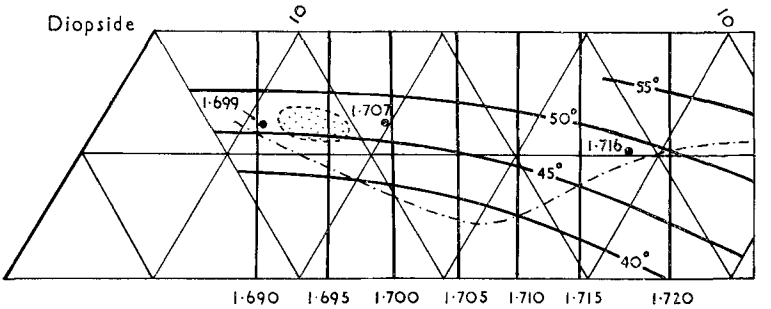

FIG. 3. Kap Edvard Holm pyroxenes plotted on the diagram constructed by Brown and Vincent (1963) showing the relationship between β-index and $2V_\gamma$ and chemical composition of the Skaergaard augite–ferroaugite series. Points labelled 1·699, 1·707, and 1·716, refer respectively to β-indices of Kap Edvard Holm pyroxenes 6, 10, and 12 (table VI). Stippled area shows the location of pyroxenes 1–5, 7–9, and 11 (tables III and VI), the β-indices of which are 1·705–1·706.

It has been noted earlier that discrepancies between the optical properties of Kap Edvard Holm and Stillwater augites are larger than those between Kap Edvard Holm and Skaergaard augites with comparable Mg:Fe ratios. The greater discrepancy which exists between the Kap Edvard Holm and Stillwater augites can be attributed to the combination of a higher Ti with a higher $[Al]^4$ content in the former, a conclusion which is compatible with Segnit's (1953) data relating to the effects of TiO_2 on the refractive indices of diopside. Although the atomic % $(Fe^{+2}+Fe^{+3}+Mn)$ of the five augites from the lower layered series increases from 12·8 to 16·3 these pyroxenes do not have significantly different refractive indices. Here, as with the Stillwater pyroxenes (Hess, 1949), the effect of the increasing replacement of Mg by Fe^{+2} on the refractive indices is neutralized by the higher content of Cr in the more magnesium-rich augites.

Cell parameters. The cell parameters of five of the lower and four of the upper layered series pyroxenes are detailed in tables III and V. The pyroxenes of both series, with the exception of 6525 (table III, no. 3), show a small progressive increase in the value of the b parameter

as the iron contents increase, and they thus conform with Brown's (1960) conclusion that b increases linearly as Mg is replaced by Fe^{+2} in the clinopyroxene structure. Estimates of the Ca:Mg:Fe^{+2} ratios for each of the pyroxenes, obtained by plotting b and $a \sin \beta$ values on the diagram constructed by Brown give higher Fe and lower Mg contents than are indicated by the chemical analyses. If, however, Fe^{+2} is replaced in the ratio by $\sum Fe^{+2}$,Fe^{+3},Mn, the estimated values approximate closely to those obtained from the chemical composition, and in general differ by less than 1·5 Fe. Thus for the Kap Edvard Holm pyroxenes the b and $a \sin \beta$ parameters are superior to the β index and $2V_\gamma$ as a guide to their composition.

The trend of the pyroxene crystallization

The pyroxenes of the Kap Edvard Holm cumulates are more Ca-rich than those of the layered series of the Skaergaard intrusion, or of those from the Tertiary acid glasses described by Carmichael (1960, 1963). They are, however, not as rich in Ca as pyroxenes which have crystallized from such alkali olivine basalt magmas as have given rise to the Garbh Eilean picrodolerite and crinanite (Murray, 1954), and the Black Jack teschenite (Wilkinson, 1956, 1957).

The compositional trends of the pyroxenes from both the lower and upper layered series is in marked contrast with that of the Skaergaard Ca-rich pyroxenes (fig. 4). The Ca contents of the Kap Edvard Holm pyroxenes show relatively little variation, amounting only to 0·5 in the lower and to 1·6 atomic % in the upper layered series. Thus the trend, like that characteristically associated with crystallization from alkali olivine basalt magmas, is essentially parallel to the diopside–hedenbergite join.

A further contrast between the Ca-rich pyroxenes of the Kap Edvard Holm and Skaergaard cumulates is the limited range in iron enrichment shown by the pyroxenes of both the lower and upper layered series of the Kap Edvard Holm complex. This is particularly marked in the upper layered series in which the total thickness of the cumulates is some 1000 m greater than the whole of the exposed layered series of the Skaergaard intrusion. Even more significant than the great difference in the range in iron enrichment shown by the pyroxenes of the Skaergaard rocks, compared with those of the upper layered series of Kap Edvard Holm, is the difference in their varying and contrasting rates of iron-enrichment. Thus the upper layered series pyroxenes show an increase from 11 to 16 atomic % Fe in the first 1300 m followed by an

increase to only 20 atomic % in the subsequent 2200 m, compared with the Skaergaard pyroxenes in which the atomic % of Fe increases from 17 to 28 % in the lower and middle zones (approximately 1500 m in thickness) and from 28 to 57 % in the upper zone (approximately 1000 m in thickness).

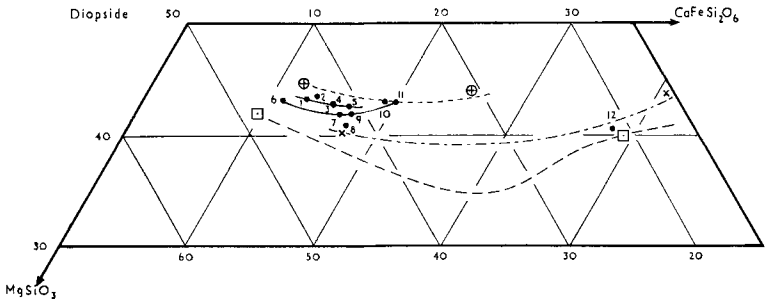

FIG. 4. Crystallization trends of the pyroxenes of the lower and upper layered series of the Kap Edvard Holm gabbro cumulates. ⊕— — —⊕ trend of the Garbh Eilean pyroxenes (Murray, 1954). ×- - - - -× trend of the calcium-rich pyroxenes from some British and Icelandic Tertiary acid glasses (Carmichael, 1960). ⊡— — —⊡ trend of the calcium-rich pyroxenes of the LZ, MZ, and UZ *a* and *b* zones of the Skaergaard intrusion (Brown, 1957; Brown and Vincent, 1963).

The contrasted trend of Ca-rich pyroxene crystallization from fractionated tholeiitic and alkali olivine basalt magmas, as characterized by the Skaergaard and Garbh Eilean intrusions, can no doubt be correlated, at least partially, with initial differences in chemical composition of the two liquids. The chilled basic magma of the Kap Edvard Holm complex, however, has not been observed and it is thus not possible to relate the contrasted trends of pyroxene crystallization in the cumulates of the Kap Edvard Holm and Skaergaard intrusions to initial differences in magmatic compositions. The composition, $Ca_{42\cdot7}Mg_{46\cdot0}Fe_{11\cdot3}$, of the pyroxene (table IV anal. 6) from the lowest rocks of the upper layered series is close to that of the augite, $Ca_{42\cdot4}Mg_{47\cdot9}Fe_{9\cdot7}$, from the Skaergaard gabbro–picrite. Furthermore, extrapolation of the crystallization trends of the upper layered series and Skaergaard Ca-rich pyroxenes to more Mg-rich compositions shows that they converge at the composition $Ca_{43\cdot5}Mg_{50}Fe_{6\cdot5}$ which is similar in composition to the early pyroxenes from other intrusions, e.g. the Bushveld complex (Hess, 1949) and the layered ultrabasic rocks of Rhum (Brown, 1956). These data are considered to indicate that the initial magmas of the Kap Edvard Holm

intrusions and Skaergaard were similar in composition; the question of the contrasted Ca-rich pyroxene crystallization thus remains.

The phase relations in the system $CaMgSi_2O_6$–$CaFeSi_2O_6$ have been determined by Schairer and Yoder (1962). The system is essentially binary for compositions between $CaMgSi_2O_6$ and those containing approximately 60 % $CaFeSi_2O_6$, and the data from natural pyroxenes indicate that comparable solid solution series containing less than one calcium atom per formula unit also occur. The mutual relationship between the solidus and liquidus curves in the synthetic system show that during the earlier stages of crystallization the composition of the liquid is enriched in iron more rapidly than the solid phase in equilibrium with the liquid, and that the rates of iron enrichment in both the liquid and solid phases reach equality when the composition of the crystals is approximately $Ca_{50}Mg_{35}Fe_{15}$. Equivalent compositions for the Kap Edvard Holm and Skaergaard Ca-rich pyroxenes are $Ca_{43}Mg_{40}Fe_{17}$ and $Ca_{38}Mg_{40}Fe_{22}$ respectively. Thus there seems little doubt that the relatively slow enrichment in iron, shown by the pyroxenes of both intrusions during the early stages of fractionation is due, at least in part, to the melting relations in the $CaMgSi_2O_6$–$CaFeSi_2O_6$ system.

The much smaller iron enrichment of the Kap Edvard Holm augites, compared with those of the Skaergaard intrusion must, however, be related to a slower rate of iron enrichment in the successive residual liquids of the Kap Edvard Holm cumulates. On this point the petrographic evidence is clear; during the crystallization of the Kap Edvard Holm liquid the precipitation of magnetite as a primary phase commenced at an earlier stage in the evolution of the Kap Edvard Holm magma, and it is present as a cumulate mineral throughout the lower layered series and in all but the lower 800 m of the upper layered series. The early formation of magnetite in the Kap Edvard Holm cumulates is also associated with the intercumulus crystallization of chlorite, amphibole, and clinozoisite. These two characteristic petrography features of the Kap Edvard Holm rocks are in marked contrast to the phase mineralogy of the Skaergaard cumulates and indicate that the crystallization of the Kap Edvard Holm liquids took place under higher water-vapour pressures, the development of which was probably the major factor in determining the different trends of crystallization shown by the two intrusions.

The Kap Edvard Holm augites do not contain exsolved lamellae of orthopyroxene and in this respect they are comparable with the clinopyroxenes of alkali basalts and related rocks. Such lamellae are also absent

from the calcium-rich pyroxenes of the Tertiary glasses investigated by Carmichael (1960). From the evidence of the extended range of iron enrichment in the orthopyroxenes, instead of the crystallization of a calcium-poor clinopyroxene (pigeonite) in these rocks, Carmichael concluded that the crystallization temperatures of the coexisting calcium-rich clinopyroxenes were likely to be lower than those at which Skaergaard augites of comparable Mg:Fe ratios crystallized. The amount of $(Mg,Fe)_2Si_2O_6$ that can be retained in solid solution in $Ca(Mg,Fe)Si_2O_6$ at sub-solvus temperatures is not known. The evidence of the experimentally determined form of the solvus in the synthetic system $MgSiO_3$–$CaMgSi_2O_6$ (Boyd and Schairer, 1962), however, indicates that augites containing smaller quantities of $(Mg,Fe)SiO_3$ in solid solution have a lower temperature of crystallization than those which initially contained larger quantities and which partially exsolved on subsequent cooling. It is unlikely that at the time of their emplacement the temperatures of the Kap Edvard Holm and Skaergaard magmas were markedly different. Thus the lower temperatures of crystallization indicated for the Kap Edvard Holm augites are most probably related to lower solidus temperatures consequent on the development of higher water-vapour pressures which prevailed during the greater part of the crystallization of the Kap Edvard Holm liquids.

It is not without significance that, although the Ca content of the pyroxenes of the lower and upper layered series are comparable, there is a small but consistent difference between the pyroxenes from the lower layered series and those from approximately the lower 2500 m of the upper layered series (fig. 4). Thus it appears that there is a correlation between the higher Ca content of the lower layered series pyroxenes and higher water-vapour pressures which, as indicated by the formation of late hydrous phases in relatively large quantities, prevailed during their crystallization. Further evidence in support of this correlation is provided by the marked increase in the Ca content of the pyroxenes (6559 and 6241) from the top 500 m of the upper layered series. These rocks also contain relatively large amounts of the late hydrous phase in strong contrast to the lower rocks of the series which are strikingly free of these minerals.

Acknowledgements. The first-named author wishes to express his indebtedness to Professor L. R. Wager for first introducing him to the rocks of the Kangerdlugssuaq region, and under whose leadership the reconnaissance mapping of the Kap Edvard Holm complex was undertaken, as part of the programme of the British East Greenland Expedition, 1935–36. He also thanks Dr. G. D. Nicholls and Dr. P. E. Brown for their help and companionship during the East Greenland Geological

Expedition, 1953, when the more detailed mapping of the complex was accomplished. Both authors are grateful to Mr. J. H. Scoon for some of the pyroxene analyses, and to Mr. R. Allen for the trace element data.

References

BOYD (F. R.) and SCHAIRER (J. F.), 1962. Carnegie Inst. Washington, Ann. Rep. Dir. Geophys. Lab., 1961–62, p. 68.
BROWN (G. M.), 1956. Phil. Trans. Roy. Soc., ser B, vol. 240, p. 1.
—— 1957. Min. Mag., vol. 31, p. 511.
—— 1960. Amer. Min., vol. 45, p. 15.
—— and VINCENT (E. A.), 1963. Journ. Petr., vol. 4, p. 175.
CARMICHAEL (I. S. E.), 1960. Journ. Petr., vol. 1, p. 309.
—— 1963. Min. Mag., vol. 33, p. 394.
HESS (H. H.), 1949. Amer. Min., vol. 34, p. 621.
—— 1960. Geol. Soc. Amer., Memoir 80.
HORI (F.), 1954. Scientific Papers, College General Education, Univ. Tokyo, vol. 4. p. 71.
MUIR (I. D.), 1951. Min. Mag., vol. 29, p. 690.
MURRAY (R. J.), 1954. Geol. Mag., vol. 91, p. 17.
SCHAIRER (J. F.), and YODER (H. S.), 1962. Carnegie Inst. Washington, Ann. Rep. Dir. Geophys. Lab., 1961–62, p. 75.
SEGNIT (E. R.), 1953. Min. Mag., vol. 30, p. 218.
TURNER (F. J.), 1947. Amer. Min., vol. 32, p. 389.
WAGER (L. R.), 1934. Meddel. om Grønland, vol. 105, no. 2.
—— 1965. Min. Mag., this vol., p. 487.
——, BROWN (G. M.) and WADSWORTH (W. J.), 1960. Journ. Petr., vol. 1, p. 73.
—— and DEER (W. A.), 1938. Geol. Mag., vol. 75, p. 39.
—— —— 1939. Meddel. om Grønland, vol. 105, No. 4.
WILKINSON (J. F. G.), 1956. Amer. Min., vol. 41, p. 724.
—— 1957. Geol. Mag., vol. 94, p. 123.
YODER (H. S.) and SAHAMA (Th. G.), 1957. Amer. Min., vol. 42, p. 475.
ZVETKOV (A. I.), 1945. Mem. Soc. Russe Min., vol. 74, p. 215.